

pubs.acs.org/acssensors Article

Microneedle-Based Potentiometric Sensing System for Continuous Monitoring of Multiple Electrolytes in Skin Interstitial Fluids

Huijie Li, Guangfu Wu, Zhengyan Weng, He Sun, Ravi Nistala, and Yi Zhang*



Cite This: ACS Sens. 2021, 6, 2181-2190



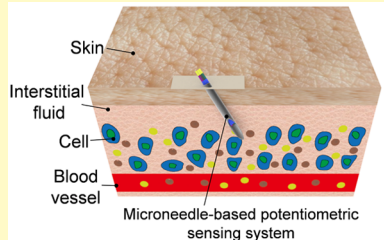
ACCESS

Metrics & More



Supporting Information

ABSTRACT: Electrolytes play a pivotal role in regulating cardiovascular functions, hydration, and muscle activation. The current standards for monitoring electrolytes involve periodic sampling of blood and measurements using laboratory techniques, which are often uncomfortable/inconvenient to the subjects and add considerable expense to the management of their underlying disease conditions. The wide range of electrolytes in skin interstitial fluids (ISFs) and their correlations with those in plasma create exciting opportunities for applications such as electrolyte





and circadian metabolism monitoring. However, it has been challenging to monitor these electrolytes in the skin ISFs. In this study, we report a minimally invasive microneedle-based potentiometric sensing system for multiplexed and continuous monitoring of Na⁺ and K⁺ in the skin ISFs. The potentiometric sensing system consists of a miniaturized stainless-steel hollow microneedle to prevent sensor delamination and a set of modified microneedle electrodes for multiplex monitoring. We demonstrate the measurement of Na⁺ and K⁺ in artificial ISFs with a fast response time, excellent reversibility and repeatability, adequate selectivity, and negligible potential interferences upon the addition of a physiologically relevant concentration of metabolites, dietary biomarkers, and nutrients. In addition, the sensor maintains the sensitivity after multiple insertions into the chicken skin model. Furthermore, the measurements in artificial ISFs using calibrated sensors confirm the accurate measurements of physiological electrolytes in artificial ISFs. Finally, the skin-mimicking phantom gel and chicken skin model experiments demonstrate the sensor's potential for minimally invasive monitoring of electrolytes in skin ISFs. The developed sensor platform can be adapted for a wide range of other applications, including real-time monitoring of nutrients, metabolites, and proteins.

KEYWORDS: interstitial fluids, minimally invasive, potentiometric biosensor, sodium, potassium

lectrolytes play a critical role in many key physicochemical functions, such as hydration, muscle activation, active membrane transport, and many others. 1-4 Electrolyte imbalances can lead to various perturbations, such as hyperkalemia, hypernatremia, hypokalemia, and hyponatremia, which in turn could lead to a range of clinical conditions such as arrhythmias, mental status changes including seizures, muscle cramps, and even death. 5,6 Currently, these conditions are diagnosed based on needed or periodic electrolyte measurements in laboratories using blood samples from patients. Such sample collection and testing procedures are uncomfortable, time-consuming, and unable to provide realtime monitoring capability. Wearable biosensors have emerged as an important platform for personalized healthcare, 8-11 in large part because these sensors are able to provide real-time pathophysiological information and measurements of biomarkers in biofluids, such as sweat, saliva, and interstitial fluids (ISFs). 12,13 Sweat analysis remains a challenging task due to the variable correlation of electrolytes in sweat with those in blood. 14,15 Tears and saliva are constrained by their limited amount of biomarkers. 13 In contrast, ISFs are formed through extravasation of plasma from continuous capillaries and surrounding tissues and cells. 16,17 Due to a combination of

factors such as the high density and surface-to-volume ratio of continuous capillaries, force produced by blood pressure, and diverse transport routes of biomarkers from plasma to ISFs, many low-molecular-weight analytes, including metabolites (glucose and lactate) and electrolytes (Na⁺, K⁺, and Ca²⁺), have similar concentrations in plasma and ISFs. Most importantly, the analysis of ISFs does not suffer from interferences by blood components and potential biofouling when compared to blood tests. Therefore, the ISFs provide a viable alternative approach to blood analysis for real-time health monitoring. 13,17-19

Skin is the largest and most accessible organ of our body, which represents a convenient and attractive source of ISFs. The skin ISFs lie in the superficial dermis, located directly beneath the epidermis, which is an optimal area for skin ISF

Received: November 6, 2020 Accepted: May 12, 2021 Published: May 26, 2021





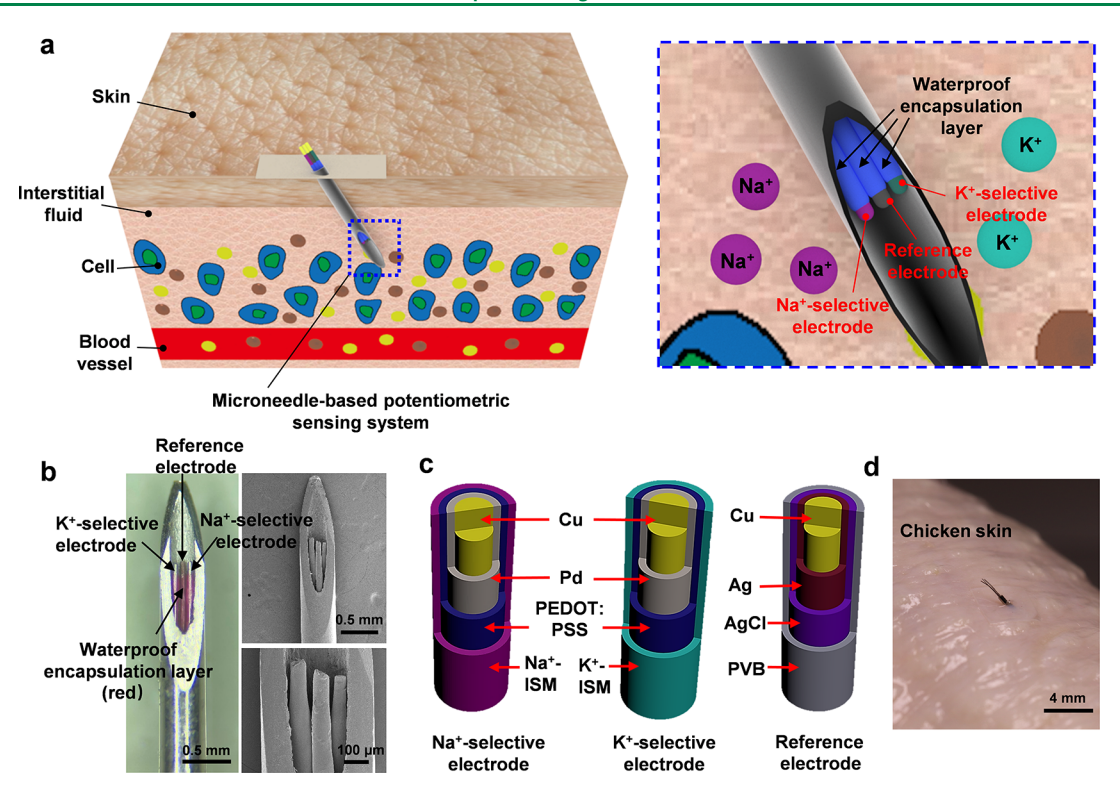


Figure 1. Microneedle-based potentiometric sensing system for simultaneous Na⁺ and K⁺ monitoring in skin ISFs. (a) Schematic illustration of the insertion of a microneedle-based potentiometric sensor into the skin (left) and the illustration of the microneedle-based potentiometric sensing system consisting of a sodium ion-selective electrode, a potassium ion-selective electrode, and an Ag/AgCl reference electrode (right). (b) Optical and scanning electron microscope images of an integrated potentiometric sensing system. The ion-selective membranes at the tip end of the electrode are separated by the waterproof encapsulation layer, thereby preventing the potential contact issue. (c) Schematic illustration of functional layers of the sodium ion-selective electrode, the potassium ion-selective electrode, and the reference electrode with multi-layer modifications. (d) Optical image of the integrated microneedle-based potentiometric sensing system when applied into a chicken skin model.

analysis since it is close enough to the capillary blood flow, thereby facilitating the transport of biomarkers from blood to skin ISFs. 17,18,20 Despite the widely available biomarkers in ISFs and the potential utility in monitoring human disease conditions, accessing the ISFs has been challenging. Existing methods used to obtain skin ISF samples include microdialysis, suction blister, and reverse iontophoresis. 21-23 These methods are usually complicated, cause patient discomfort and skin irritation, may alter the analyte concentration, and require relatively large sample volumes for benchtop instrumental analysis. Recently, there has been a growing interest in microneedle-based sensors that can penetrate through the skin to analyze the biomarkers in skin ISFs. 24-28 During the detection, the microneedles tend to avoid touching the nerve endings, thereby enabling painless monitoring of biomarkers in ISFs. The in situ analysis of skin ISF electrolytes through microneedle-based potentiometric sensors represents a promising approach due to the sensors' simple design and painless operation. 18 This microneedle potentiometric sensor, however, is still constrained by the challenge of sensor delamination when a sensor is directly inserted into the skin. Furthermore, there is a lack of a microneedle potentiometric sensor for continuous monitoring of multiple electrolytes. 25,29 Electrolyte disorders may happen coincidentally with hypomagnesemia and hypokalemia. 30,31 Hypertension management is normally based on the monitoring of the salivary potassium/sodium ratio. 32,33 In addition, the level of electrolytes may fluctuate throughout the day due to diet, exercise, or disease.³⁴ Thus, it is important to develop a mechanically robust and multiplexed

microneedle-based potentiometric sensor for continuously monitoring multiple electrolytes for timely diagnosis and monitoring of various disease conditions.

In this study, we developed a minimally invasive microneedle-based potentiometric sensing system for monitoring multiple electrolytes from skin ISFs. The new biosensor demonstrates an attractive analytical performance with a fast response time, excellent reversibility and repeatability, as well as adequate selectivity for ISF Na⁺ and K⁺ analysis. In addition, the mechanical stability of the developed potentiometric sensors with the hollow microneedle structure was evaluated by inserting the integrated sensors into chicken skin multiple times. Furthermore, our experiments, which measured the concentration of Na+ and K+ in skin-mimicking phantom gel and chicken skin model, highlight the potential applications for minimally invasive and real-time monitoring of electrolytes in skin ISFs. The developed sensor platform can be adapted for the real-time monitoring of nutrients, metabolites, and proteins.

■ EXPERIMENTAL SECTION

Materials. The copper wire (diam. 0.05 mm), acetone, potassium chloride (KCl), sodium chloride (NaCl), platinum (Pt) wire (diam. 0.25 mm), silver (Ag) wire (diam. 2 mm), isopropyl alcohol, hydrochloric acid, sodium ionophore X, bis (2-ethylhexyl) sebacate (DOS), sodium tetrakis [3,5-bis(trifluoromethyl)phenyl] borate (NaTFPB), polyvinyl chloride (PVC), tetrahydrofuran (THF), valinomycin (potassium ionophore), polyvinyl butyral (PVB), 3,4-ethylenedioxythiophene (EDOT), and poly (4-styrenesulfonic acid) solution (PSS) were purchased from Sigma Aldrich. Palladium (Pd)

plating solution and non-cyanide Ag plating solution were obtained from Rio Grande. The artificial ISF (2.5 mM CaCl₂, 5.5 mM glucose, 10 mM Hepes, 3.5 mM KCl, 0.7 mM MgCl₂, 123 mM NaCl, 1.5 mM NaH₂PO₄, and 7.4 mM sucrose) was prepared according to the published literature. 35,36 Commercial sodium and potassium testers (NA-11 LAQUAtwin Na-11 Pocket Tester and B-731 Potassium LAQUAtwin K-11 Pocket Tester) were purchased from HORIBA Ltd., Japan. Chicken skin was purchased from a local market. The pH of the artificial ISF was adjusted to 7.4. Ultra-pure deionized water (18.2 M Ω cm) was used to prepare all samples.

Preparation and Cleaning of Copper Wires. We used copper wires as the primary elements for preparing ion-selective electrodes. Prior to use, copper wires were cleaned by rinsing with acetone, isopropyl alcohol, and diluted hydrochloric acid, followed by ultrasonic agitation with deionized water for 5 min. Multiple copper wires (10–15) were placed in parallel with a spacing of approximately 1 mm on a strip of conductive silver tape and then placed (adhesive side facing inward) on the head of a custom-made "n" wire plastic holder to allow for lifting all wires simultaneously (Figure S1).

Electroplating of Pd on Copper Wires. Pd electroplating onto the above-prepared copper wires was performed by using a two-electrode cell at 50 °C in a Pd plating solution. A Pt wire, which served as the counter electrode, was attached to the positive (+) lead and immersed in solution. The prepared copper wires were electrically connected to the negative (-) lead as the working electrodes using the previously attached conductive tape. Operation at a 3 mA cathodic current and 2.6 V for 30 min completed the Pd electroplating.³⁷

Coating of PEDOT:PSS. As an ion-electron transducer between the ion-selected membrane and the electroplated copper wires, PEDOT:PSS was coated on the Pd-electroplated copper wires through electrochemical polymerization. PEDOT:PSS solution was prepared by mixing 0.1 wt % EDOT and 4 wt % PSS in deionized water with ultrasonication for 5 min. Working electrodes were coated with a PEDOT:PSS layer by electropolymerization carried out with a Metrohm Autolab-PGSTAT128N. More specifically, we increased the applied potential from 0.4 to 0.9 V in five steps, and then held the potential of 0.9 V for 40 s. This electropolymerization protocol was repeated twice, and then the obtained electrodes were cured at 65 °C for 3 h.38 The length of the PEDOT:PSS layer on the Pdelectroplated copper wire is about 2 cm. For the potentiometric measurement, the electrode modified with PEDOT:PSS proved to be more stable and demonstrated a better linear relationship when compared to those without PEDOT:PSS modification (Figure S2).

Coating of Na+- and K+-Selective Membranes. The ionselective membrane was prepared as described previously.³⁹ Briefly, the Na+-selective membrane cocktail was composed of Na ionophore X (1% w/w), Na-TFPB (0.55% w/w), DOS (65.45% w/ w), and PVC (33% w/w). We then dissolved 100 mg of the membrane cocktail in 660 μ L of THF. We prepared the K⁺selective membrane cocktail with the composition of valinomycin (2% w/w), Na-TFPB (0.5% w/w), PVC (32.75% w/w), and DOS (64.75% w/w). 100 mg of the prepared membrane cocktail was dissolved in 700 μ L of THF.⁴³ The cocktails were vigorously mixed for 2 min by using a Vortex Mixer and then sealed and stored at 4 °C. Two microliters of the membrane cocktail were drop-casted on the surface of the working electrodes five times with a length of about 1 cm and dried at room temperature for at least 8 h. We painted the dried ion-selective electrodes with nail polish to form a waterproof encapsulation layer by using a small brush, leaving ~ 0.2 mm of the ion-selective membrane uncovered at the tip end44 (Figures 1 and S1). With such a strategy, the waterproof encapsulation layer prevents the ion-selective membranes from touching each other. In the meanwhile, the ion can reach the ion-selective membrane through these uncovered areas. Finally, the encapsulated electrodes were placed in the solution of target ions (0.1 M of NaCl or KCl) overnight.⁴⁵ The diameters of the prepared Na⁺- and K⁺-selective electrodes were characterized using a scanning electron microscope (FEI Nova NanoSEM 450).

Preparation of the Ag/AgCl Reference Electrode. The reference electrode was prepared as described previously.3 Briefly, the electroplating of Ag onto clean copper electrodes was achieved by using a two-electrode cell at room temperature in an Ag plating solution. An Ag wire, which served as the counter electrode, was attached to the positive (+) lead and immersed in the solution. The cleaned copper wires were electrically connected to the negative (-) lead as the working electrodes using the previously placed conductive tape. The power supply was operated at an 8 mA cathodic current and 1.62 V for 5 min. The electroplating of AgCl onto the above Ag-electroplated copper wire was achieved by using a twoelectrode cell at room temperature in 0.1 M KCl solution. The Ag wire was attached to the negative (-) lead and immersed in the KCl solution, and the Ag-electroplated copper wires were used as the working electrodes. A power supply of 3 mA anodic current and 2.1 V was used for 1 min. The length of the electroplated AgCl layer was \sim 5 mm. We prepared the PVB solution by dissolving 79.1 mg of PVB and 50 mg of NaCl into 1 mL of methanol.⁴⁸ The above-prepared Ag/ AgCl reference electrode was then coated with PVB to obtain a stable potential among a wide range of ion concentrations.⁴⁸ Finally, the prepared Ag/AgCl reference electrode was encapsulated with a nail polish layer, leaving an ~0.2 mm tip end uncovered. The diameters of the prepared reference electrodes were characterized using a scanning electron microscope (FEI Nova NanoSEM 450).

Device Assembly. A hollow microneedle with a length of 4 mm was created from a 26-gauge hypodermic needle (outer diameter: 0.464 mm, inner diameter: 0.260 mm) using a milling machine. A layer of polydimethylsiloxane (PDMS) was used as a substrate to support the hollow microneedle during the operation. Here, the Na⁺-selective electrode, and Ag/AgCl reference electrode were carefully and gently inserted one after another into the hollow microneedle fixed to a PDMS substrate under a microscope. The position of electrodes in the hollow microneedle was adjusted under the microscope.

Electrochemical Characterizations. All electrochemical characterizations of the Na⁺ and K⁺ sensors were performed on an Autolab PGSTAT128N potentiostat (Metrohm). The PVB-modified Ag/AgCl electrode was used as a reference electrode, and the Na⁺-selective electrode and K⁺-selective electrode were used as working electrodes. The open-circuit potential (OCP) was recorded (vs Ag/AgCl reference electrode) after 5 s of holding in the sample solution. ^{49–52}

■ RESULTS AND DISCUSSION

Microneedle-Based Potentiometric Sensing System for Skin ISF Analysis. The microneedle-based potentiometric sensing system includes the following two key components: (1) a miniaturized stainless-steel hollow microneedle (26gauge) to prevent sensor delamination during insertion and (2) a set of microneedle-based potentiometric sensors for multiplex monitoring of Na+ and K+ in skin ISFs (Figure 1ac). It should be noted that the stainless-steel hollow microneedle we used was only 26 gauge (outer diameter was 0.464 mm). In routine blood collection, a 21-gauge (outer diameter is 0.819 mm) needle is often used.⁵³ To the best of our knowledge, the smallest sensor needle for commercial continuous glucose meters (CGMs) is 26 gauge.⁵⁴ For example, Medtronic's needles are 23 gauge (MiniMed Paradigm REAL-Time Revel) and Dexcom's needles are 26 gauge. Therefore, our sensors have the potential to monitor biomarkers in a minimally invasive manner like CGMs. We used a micrometer-scale copper wire (50 μ m) as the primary electrode element to prepare the potentiometric electrodes by electroplating and dip-coating of functionalized layers. More specifically, the working electrodes were prepared by electroplating Pd and PEDOT:PSS onto the copper wire, followed by the functionalization with ion-selective membranes (Figures 1c and S3). This preparation process does not involve

complicated and expensive microfabrication equipments. Figure 1c schematizes all the functional coatings used for the preparation of the microneedle-based Na⁺- and K⁺-selective electrodes and the reference electrode. Figures S3 and S4 show the SEM images of the ion-selective electrodes and Ag/AgCl reference electrode, indicating that the copper wires are coated with functional layers. As shown in Figure S5, the total diameters of the sodium ion-selective electrode, potassium ionselective electrode, and Ag/AgCl reference electrode are approximately 91.2, 89.3, and 92.2 µm with relative standard deviations (RSDs) of 7.12, 5.09, and 3.77%, respectively. These three functionalized electrodes are then integrated into the hollow microneedle (Figure 1a,b). No damage is observed for these electrodes after inserting them into the hollow microneedle five times, as shown in Figure S6. The hollow microneedle protects the electrodes from delamination during the insertion and facilitates ISF access via painless skin penetration. It should be noted that these electrodes are housed at the opening aperture of the hollow microneedle (Figure 1a,b), thereby enabling the direct contact of the electrodes with the ISF and achieving the real-time monitoring of fluctuations in electrolyte concentrations. An optical image of a microneedle-based potentiometric sensing system compared with a 0.35 mm puncher is shown in Figure S7. Figure 1d shows an optical image of a microneedle-based potentiometric sensor mounted on a chicken skin model for electrolyte monitoring. Importantly, based on previous studies, ion-selective electrodes can be used in vivo for at least 24 h,25,55 indicating the potential for continuous monitoring in in vivo studies.

Electrochemical Characterization of Reference Elec**trodes.** The solid-state reference electrode is prepared by electroplating Ag and AgCl successively onto the copper wire, followed by drop-casting the membrane cocktail of PVB onto the electrode. The PVB membrane cocktail is vital for maintaining a constant potential.⁴⁸ The PVB-coated solidstate Ag/AgCl reference electrode shows a stable potential in different NaCl solutions (Figure 2a). We fabricate two types of solid-state reference electrodes, one with the Ag/AgCl electrode (prepared by chloritization of Ag wire) and another one with a copper wire functionalized with Ag and Ag/AgCl through electroplating methods (Figure S4). These solid-state electrodes made by electroplating Ag/AgCl on the Cu wire demonstrate significantly improved stability, rapid response time, and high reproducibility (Figure 2b,c). In contrast, the reference electrode made with chloritization of Ag wire exhibits potential fluctuations in low concentrations of Na⁺ (5-50 mM) (Figure 2b). Therefore, we use the copper wire-based Ag/AgCl electrode as the reference electrode for our experiments. Both working and reference electrodes are encapsulated by a waterproof nail polish layer (Figure 1b; labeled with a red dye), leaving only 0.2 mm of the electrode uncovered at the tip end. This encapsulation layer separates each electrode and prevents the potential contact of each electrode, thereby avoiding the mixed potential issue. Figure 2d shows the negligible potential fluctuations of OCP responses with different concentrations of Na+ when the working and reference electrodes are physically separated (black curve) and assembled into the hollow microneedle (red curve). We also performed additional experiments to investigate the signal interferences caused by introducing an additional ion-selective electrode (Figure S8). There is no significant change in the sensor's sensitivity when introducing

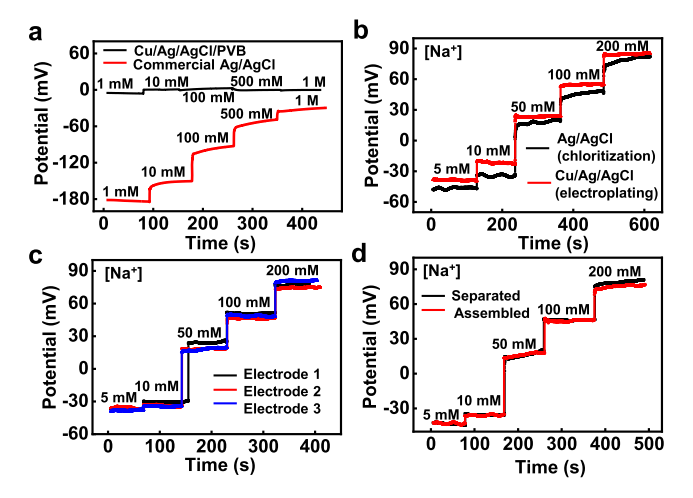


Figure 2. Electrochemical characterizations of reference electrodes. (a) Potential stability of a commercial Ag/AgCl electrode and a PVB-modified Cu/Ag/AgCl electrode in different NaCl solutions. (b) OCP curves of an Ag wire decorated with silver chloride and a copper wire functionalized with Ag and AgCl in various concentrations of NaCl. (c) Reproducibility of reference electrodes (Cu/Ag/AgCl) (n = 3). (d) Comparison of the electrochemical performance of the working electrode and reference electrode when they are physically separated (black line) and when assembled into a hollow microneedle (red line).

an additional ion-selective electrode to the existing ion-selective electrode because the waterproof encapsulation layer can prevent the contact of ion-selective membranes (as shown Figure 1b), indicating capability for multiplex monitoring.

Electrochemical Performance of a Potentiometric Na⁺ Sensor in Artificial ISFs. The Na⁺ sensor is first functionalized by electroplating Pd onto a core copper wire, followed by electropolymerization of PEDOT:PSS, which is then modified with a sodium ionophore X-based PVC membrane cocktail, and finally dried at room temperature overnight. After the selective encapsulation with a nail polish layer, the Na⁺-selective electrode is immersed into a solution containing 0.1 M NaCl for at least 8 h before the measurements to minimize potential drift. Finally, the prepared Na⁺-selective electrode is inserted into a stainless hollow microneedle to finish the preparation of a Na⁺ sensor.

To evaluate the performance of the Na⁺ sensor, the sensor is tested in artificial ISFs containing a physiologically relevant concentration of NaCl ranging from 0 to 200 mM. 18,56 The calibration curve is obtained by recording the OCP versus time (Figure 3a). As shown in the insets of Figure 3a, there is a clear linear relationship between the OCP and the logarithm of Na⁺ concentration. The slope is 56.08 mV/decade, showing a near Nernstian response (sensitivity: 59 mV/decade), and the linear correlation coefficient (R²) is 0.991 for the Na⁺ sensor. This suggests that the prepared Na+ sensor has the potential to quantitatively detect Na⁺ in artificial ISFs. Figure 3b shows the result of a carry-over test by increasing and decreasing the concentration of Na+, demonstrating that the Na+ sensor follows rapid fluctuation of electrolytes levels within the physiological range of Na⁺ (0-200 mM) in artificial ISFs. This potential-time trace reveals that the OCP of the sensor changes along with the increasing/decreasing of Na⁺ concentration in artificial ISFs and that the sensor responds instantaneously to

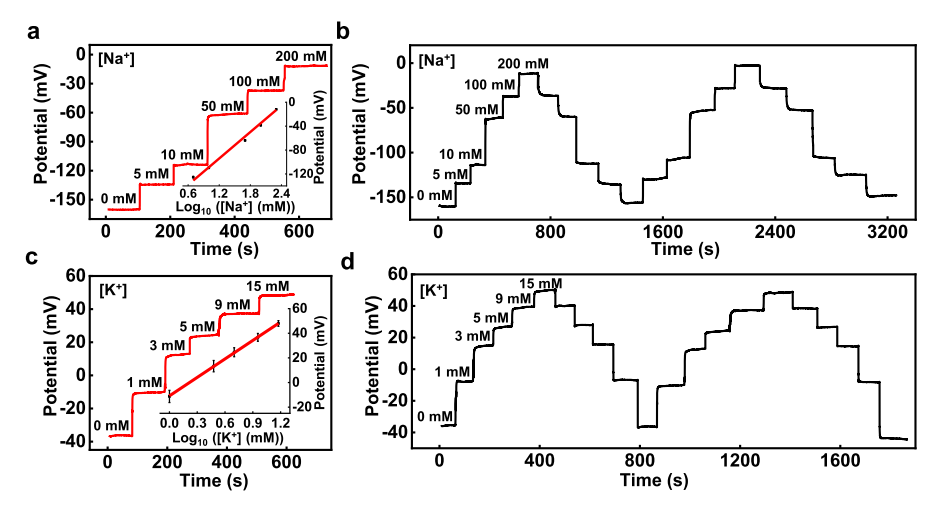


Figure 3. Electrochemical performance of Na⁺ and K⁺ sensors in artificial ISFs. (a) Response of a Na⁺ sensor to different concentrations of Na⁺ in artificial ISFs. The inset shows a linear relationship between the OCP and the logarithm of Na⁺ concentrations in artificial ISFs (n = 5). Sensitivity: 56.08 mV/decade; R^2 : 0.991. (b) Carry-over study for the Na⁺ sensor using Na⁺ with various concentrations in artificial ISFs. (c) Response of a K⁺ sensor to various concentrations of K⁺ in artificial ISFs. The inset shows a linear relationship between the OCP and the logarithm of K⁺ concentration in artificial ISFs (n = 5). Sensitivity: 50.03 mV/decade; R^2 : 0.999. (d) Carry-over study for the K⁺ sensor using various concentrations of K⁺ in artificial ISFs.

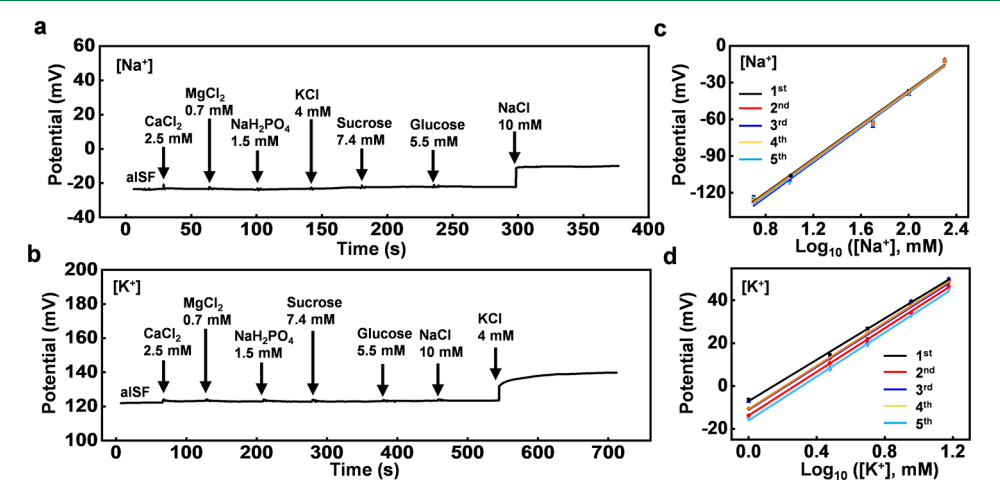


Figure 4. Selectivity and repeatability of potentiometric Na^+ and K^+ sensors. The selectivity study for the (a) Na^+ sensor and (b) K^+ sensor in response to different input interferences, including $CaCl_2$, $MgCl_2$, NaH_2PO_4 , sucrose, glucose, KCl, and NaCl. The repeatability of the (c) Na^+ sensor and (d) K^+ sensor.

the amplitude change in concentrations of Na⁺, indicating the potential for real-time monitoring of Na⁺ in skin ISFs.

Electrochemical Performance of Potentiometric K⁺ **Sensor in Artificial ISFs.** Similar to the Na⁺ sensor, the K⁺ sensor is successively electrodeposited with Pd and PEDOT:PSS layers onto a copper wire and then drop-casted with a valinomycin-based PVC membrane. Finally, the prepared electrodes are dried at room temperature overnight. K⁺-selective electrode is then immersed into a solution of 0.1 M KCl for at least 8 h before the measurements to minimize potential drift. Electrochemical characterization is performed by utilizing different concentrations of KCl in a background of artificial ISF. Figure 3c demonstrates the increase in OCP of the K⁺ sensor with the increase in KCl concentration in the physiologically relevant range of 0-15 mM in artificial ISF. As shown in the inset of Figure 3c, there is a linear relationship $(R^2 = 0.999, a slope of 50.03 \text{ mV/decade})$ between the OCP and the logarithm of K+ concentration. To demonstrate that the K⁺ sensor is able to rapidly track fluctuations of electrolytes

levels, a carry-over test is performed by increasing and decreasing the K^+ concentration (0–15 mM) in the artificial ISF solution (Figures 3d). This potential-time trace suggests that the sensor responds instantaneously to the amplitude change of K^+ . These electrochemical characterizations demonstrate the capability of the prepared potentiometric K^+ sensor for real-time monitoring of K^+ changes in the skin ISF. The Na $^+$ and K^+ sensor data show that the potentiometric sensor exhibits rapid responses and negligible carry-over effects for different ion concentration levels (within the physiological range). Sensors for other ions, such as pH, Ca^{2+} , Mg^{2+} , and Cl^- , could also be prepared using a similar fabrication method.

Selectivity, Repeatability, Reversibility, and Stability of Potentiometric Na⁺ and K⁺ Sensors. The ISF is a complex body fluid containing a variety of components that may induce interferences to the potentiometric responses of Na⁺ and K⁺ sensors. To study the influence of possible interfering compounds on the sensors' response, we investigate the selectivity of Na⁺ and K⁺ sensors. More specifically, the

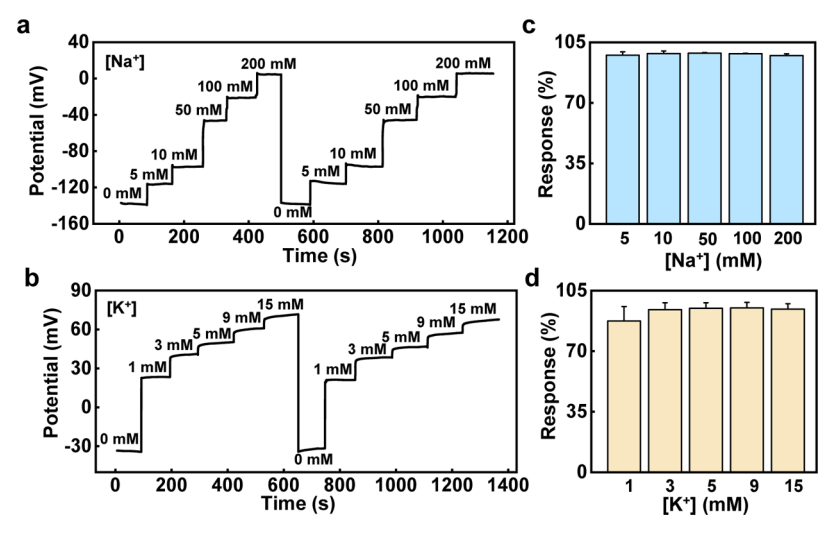


Figure 5. Reversibility of potentiometric Na^+ and K^+ sensors. The reversibility of the (a) Na^+ sensor and (b) K^+ sensor. (c) and (d) Percent of the signal return compared with its first response for Na^+ and K^+ sensors at various concentrations of NaCl and KCl, respectively (n = 5).

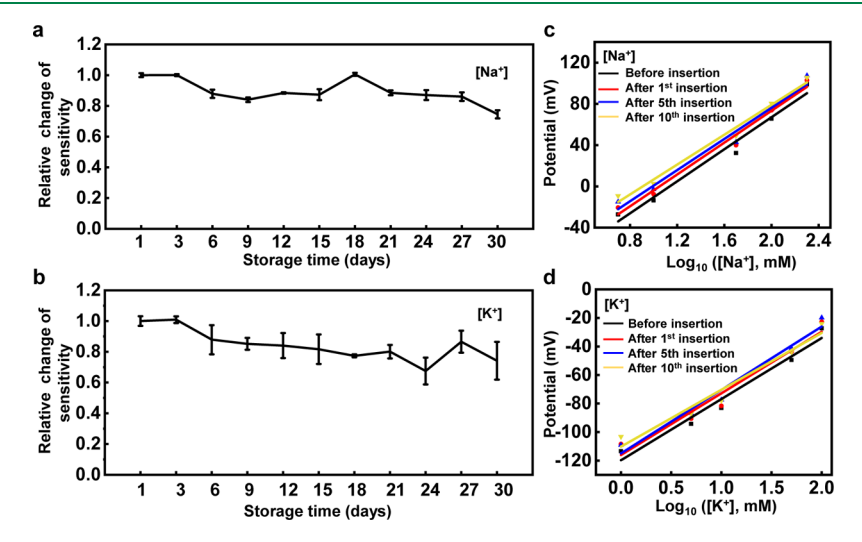


Figure 6. Storage stability and mechanical durability of potentiometric Na⁺ and K⁺ sensors. Relative changes of sensitivity for (a) Na⁺ and (b) K ⁺ sensors, respectively. The sensitivities are measured every 3 days over a period of 30 days in artificial ISFs (n = 5). Mechanical stabilities of (c) Na⁺ and (d) K⁺ sensors, respectively. The OCPs are recorded before and after several insertions into the chicken skin.

OCP is recorded upon the addition of physiologically relevant interfering species, including KCl (4 mM), NaCl (10 mM), CaCl₂ (2.5 mM), MgCl₂ (0.7 mM), NaH₂PO₄ (1.5 mM), sucrose (7.4 mM), and glucose (5.5 mM), into the artificial ISF. Figure 4a,b shows that the potential signal changes caused by interfering ions are negligible; a similar result is observed upon the addition of physiologically relevant concentrations of clinically important metabolites (creatine and uric acid), a dietary biomarker (caffeine), and nutrients (glutamine and vitamin A) (Figure S9). These studies suggest that the developed Na+ and K+ sensors have high selectivity toward various electrolytes, metabolites, a dietary biomarker, and nutrients that are frequently found in ISFs, 19 enabling the construction of a multiplexed sensing system. Here, a difference in response time for Na⁺ and K⁺ sensors is observed, which may be attributed to the differences in the molecular weights of Na⁺ and K⁺. The sodium ion has a lower molecular weight than that of potassium, thereby causing a faster diffusion into the ion-selective membrane and formation of a sodium-ionophore complex.

Repeatability is essential for wearable sensors. By repeating the measurement five times using the same sensor, we studied the repeatability of the Na+ and K+ sensors within the biologically relevant range of Na⁺ and K⁺ concentrations in artificial ISFs (Figure 4c,d). Besides repeatability, the reversibility of the sensor's response is also critical since the potentiometric sensing system needs to be able to monitor 'positive and negative" fluctuations of electrolyte concentration in skin ISFs. This feature has been demonstrated through carry-over tests (Figure 3b,d). Here, the reversibility is further verified by evaluating the Na⁺ and K⁺ sensors' responses to the slowly increasing and rapidly decreasing concentrations of NaCl and KCl in the artificial ISF, respectively (Figure 5a,b). Figure 5c,d shows the percent of the signal return compared with its initial value for the Na⁺ and K⁺ sensors. In summary, the developed potentiometric Na⁺ and K+ sensors are stable and repeatable with a negligible potential drift. Moreover, they rapidly respond to variations in Na⁺ and K⁺ concentrations.

It is also very important to study the stability and storage lifetime of wearable biosensors. To this end, we investigate the

long-term storage stability of Na⁺ and K⁺ sensors by monitoring the sensor's sensitivity in the artificial ISF every 3 days over 30 days. Figure 6a,b shows the relative changes of sensitivity of Na+ and K+ sensors over 30 days. These results demonstrated the relatively stable operation of both sensors over 30 days, indicating the potential for long-term monitoring. The mechanical stability of developed potentiometric sensors with the hollow microneedle structure is further evaluated by inserting the integrated sensors into chicken skin multiple times. Before the first insertion into chicken skin, we obtain the OCP by testing the sensors in different concentrations of NaCl (5-200 mM) and KCl (1-100 mM) in the artificial ISF (Figure 6c,d). This process is repeated for 1, 5, and 10 insertions into the chicken skin. The RSDs of the sensor's sensitivity are 3.12% for Na⁺ and 4.55% for K⁺ sensors, demonstrating a good mechanical stability of the sensors.

Evaluation of Sensor Accuracy in Artificial ISFs. One of the major limitations of the developed microneedle-based potentiometric sensing system is its low sensor-to-sensor reproducibility (E^0) for sensors from different fabrication batches mainly due to variations caused by manual dropcasting of ion-selective membranes, which requires a sensor calibration before the analysis of electrolytes in skin ISFs. 50,57,58 To evaluate the sensor accuracy after the calibration, we first fabricate the microneedle-based potentiometric sensing system and calibrate the sensors in artificial ISFs containing a physiological range of Na $^+$ and K $^+$. Figure 7a,b

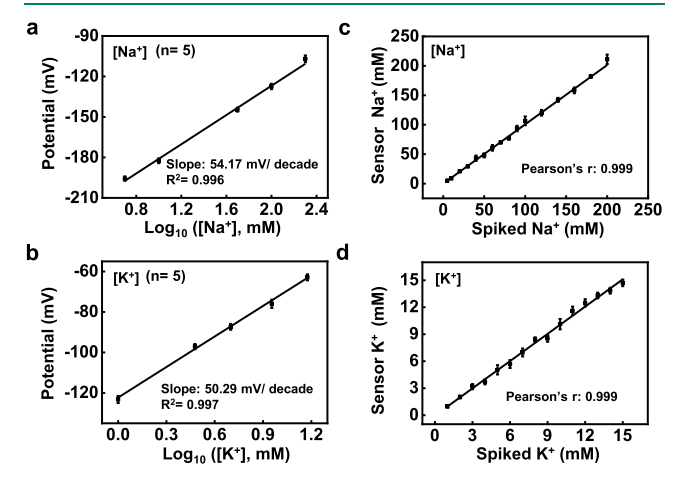


Figure 7. Evaluation of sensor accuracy. The calibration curve of microneedle-based potentiometric (a) Na^+ and (b) K^+ sensors. Comparison of (c) Na^+ and (d) K^+ measured from microneedle-based potentiometric sensors with those of spiked ion concentrations in artificial ISFs.

shows the calibration curves of microneedle-based potentiometric biosensing systems. We then perform the measurements in artificial ISFs with known concentrations of $\mathrm{Na^+}$ and $\mathrm{K^+}$ using these calibrated sensors. The values measured with the calibrated potentiometric sensors show agreement with spiked ion concentrations in artificial ISFs (Figure 7c,d), confirming the accurate measurements of physiological electrolytes in artificial ISFs.

Validations in Skin-Mimicking Phantom Gel and Chicken Skin Models. To further demonstrate the potential applications of microneedle-based potentiometric sensors, we evaluate their performance by measuring Na⁺ and K⁺ concentrations in skin-mimicking phantom gels⁵⁹ (1 wt %

agarose, Figure S10a). The phantom gels are conditioned with a known concentration of Na $^+$ or K $^+$ overnight. We first collect the ISF in phantom gels using a custom-made hollow microneedle system 60 and then measure the Na $^+$ and K $^+$ concentrations in these conditioned gels by using commercial sodium and potassium testers (HORIBA Ltd., Japan). In the meantime, a pre-calibrated microneedle-based potentiometric sensor is manually inserted into the skin-mimicking phantom gel and the OCP is recorded in triplicate. As shown in Figures 8a,b and S10b,c, the Na $^+$ and K $^+$ concentrations in phantom

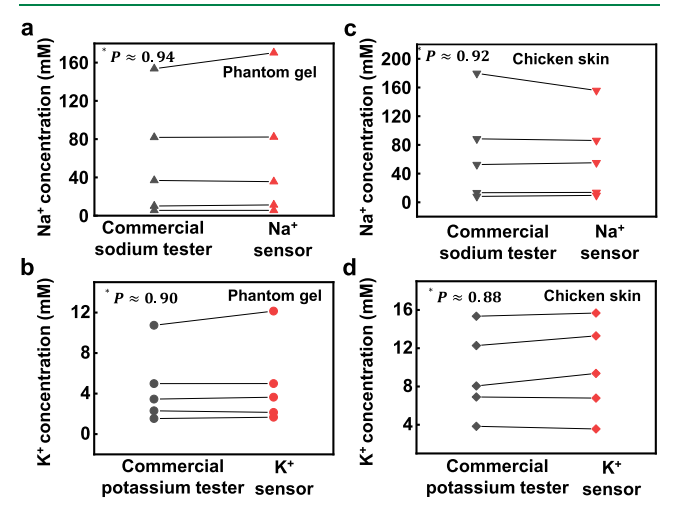


Figure 8. Validation studies using skin-mimicking phantom gel and chicken skin models. (a-d) Concentrations of sodium and potassium ions obtained using the microneedle-based potentiometric sensing system versus a commercial diagnostic instrument and the standard ISF collection method. *P < 0.01, two-tailed test.

gels, obtained by using our microneedle-based potentiometric sensing system, exhibit good correlation to those determined by commercial sodium and potassium testers. The performance of the integrated potentiometric sensing system is further assessed by detecting the Na+ and K+ levels in a chicken skin model conditioned with known concentrations of Na⁺ or K⁺ (Figure S10d). Similar to the phantom gel model, the Na⁺ and K⁺ concentrations in conditioned chicken skins are measured by using both our microneedle-based potentiometric sensing system and commercial sodium and potassium testers (as shown in Figures 8c,d and S10e and f). Overall, these validation experiments in both skin-mimicking phantom gel and chicken skin models indicate that the developed microneedle-based potentiometric sensor has the potential suitability to access both Na+ and K+ concentrations in skin ISFs in future in vivo studies.

CONCLUSIONS

In summary, we have developed a microneedle-based potentiometric sensing system that consists of a sodium ion-selective electrode, a potassium ion-selective electrode, and an Ag/AgCl reference electrode in combination with a stainless-steel hollow microneedle. The new biosensor has demonstrated an attractive analytical performance with a fast response time, excellent reversibility and repeatability, adequate selectivity, and negligible potential interference for monitoring Na⁺ and K⁺ in artificial ISFs. The developed potentiometric sensors with a hollow microneedle structure prevent sensor delamination during insertion, thereby allowing for mechan-

ically robust operation in in vivo monitoring. The phantom gel and chicken skin model experiments indicate that this potentiometric sensor provides a promising method for minimally invasive and continuous monitoring of multiple electrolytes in skin ISFs. Further work is needed to investigate and improve the long-term biocompatibility of the ionselective membrane by using biocompatible ionophores, plasticizers and hydrogel coatings, 55,61 and chemical modifications of ion-selective membranes. 62 We will also integrate the potentiometric sensing system with a mobile sensor data collection system via wireless Bluetooth communication⁶³ and evaluate the efficiency and functional robustness of devices in future in vivo studies. Such developments could lead to a wearable, minimally invasive sensing system for real-time monitoring of an individual's physiological biomarkers with high data fidelity. In addition, this sensor design can be readily adapted to a wide range of applications, including the continuous monitoring of metabolites, nutrients, and proteins.

ASSOCIATED CONTENT

Supporting Information

The Supporting Information is available free of charge at https://pubs.acs.org/doi/10.1021/acssensors.0c02330.

Fabrication process for microneedle-based potentiometric sensors; the electrode modified with PEDOT:PSS proved to be more stable when compared to those without PEDOT:PSS modification; SEM images of sodium and potassium ion-selective electrodes after each step of functionalization; SEM images of a reference electrode after each step of functionalization; the diameters of sodium ion-selective electrodes, potassium ion-selective electrodes, and reference electrodes after each step of functionalization; SEM images of the tip end of a sodium ion-selective electrode and a potassium ion-selective electrode after inserting into a hollow microneedle five times; an optical image of a microneedle-based potentiometric sensing system compared with a 0.35 mm puncher; experiments to investigate the signal interferences caused by introducing an additional ion-selective electrode; selectivity of potentiometric Na+ and K+ sensors in response to different input interferences, including creatine, uric acid, glutamine, caffeine, and vitamin A; and statistical analysis of validation studies using skin-mimicking phantom gel and chicken skin models (PDF)

AUTHOR INFORMATION

Corresponding Author

Yi Zhang — Department of Biomedical Engineering, Institute of Materials Science, University of Connecticut, Storrs, Connecticut 06269, United States; orcid.org/0000-0002-0907-663X; Email: yi.5.zhang@uconn.edu

Authors

Huijie Li — Department of Biomedical Engineering, Institute of Materials Science, University of Connecticut, Storrs, Connecticut 06269, United States

Guangfu Wu – Department of Biomedical Engineering, Institute of Materials Science, University of Connecticut, Storrs, Connecticut 06269, United States Zhengyan Weng — Department of Biomedical Engineering, Institute of Materials Science, University of Connecticut, Storrs, Connecticut 06269, United States

He Sun – Department of Biomedical Engineering, Institute of Materials Science, University of Connecticut, Storrs, Connecticut 06269, United States

Ravi Nistala – Division of Nephrology, Department of Medicine, University of Missouri-Columbia, Columbia, Missouri 65212, United States

Complete contact information is available at: https://pubs.acs.org/10.1021/acssensors.0c02330

Funding

This work was supported by the University of Connecticut start-up fund and the National Science Foundation grants (ECCS-2113736 and CBET-2103025) to Dr. Yi Zhang.

Notes

The authors declare no competing financial interest.

■ ACKNOWLEDGMENTS

We thank Ghassan Al Bahhash, the Research Engineering Technician, for helping us prepare the stainless hollow microneedles in the machine shop at the University of Missouri, Columbia.

REFERENCES

- (1) Lee Hamm, L.; Hering-Smith, K. S.; Nakhoul, N. L. Acid-base and potassium homeostasis. *Semin. Nephrol.* **2013**, *33*, 257–264.
- (2) Terry, J. The major electrolytes: sodium, potassium, and chloride. J. Intraven. Nurs. 1994, 17, 240-247.
- (3) Winston, A. P. The clinical biochemistry of anorexia nervosa. *Ann. Clin. Biochem.* **2012**, 49, 132–143.
- (4) Piccoli, G. B.; Capobianco, M.; Odetto, L.; Deagostini, M. C.; Consiglio, V.; Radeschi, G. Acute renal failure, severe sodium and potassium imbalance and sudden tetraplegia. *NDT Plus* **2010**, *3*, 247–252.
- (5) Leier, C. V.; Dei Cas, L.; Metra, M. Clinical relevance and management of the major electrolyte abnormalities in congestive heart failure: hyponatremia, hypokalemia, and hypomagnesemia. *Am. Heart J.* **1994**, 128, 564–574.
- (6) Von Duvillard, S. P.; Braun, W. A.; Markofski, M.; Beneke, R.; Leithäuser, R. Fluids and hydration in prolonged endurance performance. *Nutrition* **2004**, *20*, 651–656.
- (7) Hohmann, C.; Pfister, R.; Kuhr, K.; Merkle, J.; Hinzmann, J.; Michels, G. Determination of Electrolytes in Critical Illness Patients at Different pH Ranges: Whom Shall We Believe, the Blood Gas Analysis or the Laboratory Autoanalyzer? *Crit. Care Res. Pract.* **2019**, 2019, 9838706.
- (8) Rao, Z.; Ershad, F.; Almasri, A.; Gonzalez, L.; Wu, X.; Yu, C. Soft Electronics for the Skin: From Health Monitors to Human-Machine Interfaces. *Adv. Mater. Technol.* **2020**, *5*, 2000233.
- (9) Zhou, Z.; Chen, K.; Li, X.; Zhang, S.; Wu, Y.; Zhou, Y.; Meng, K.; Sun, C.; He, Q.; Fan, W.; Fan, E.; Lin, Z.; Tan, X.; Deng, W.; Yang, J.; Chen, J. Sign-to-speech translation using machine-learning-assisted stretchable sensor arrays. *Nat. Electron.* **2020**, *3*, 571–578.
- (10) Sempionatto, J. R.; Jeerapan, I.; Krishnan, S.; Wang, J. Wearable Chemical Sensors: Emerging Systems for On-Body Analytical Chemistry. *Anal. Chem.* **2020**, *92*, 378–396.
- (11) Yang, Y.; Gao, W. Wearable and flexible electronics for continuous molecular monitoring. *Chem. Soc. Rev.* **2019**, 48, 1465–1491
- (12) Yu, Y.; Nyein, H. Y. Y.; Gao, W.; Javey, A. Flexible Electrochemical Bioelectronics: The Rise of In Situ Bioanalysis. *Adv. Mater.* **2020**, *32*, 1902083.

- (13) Kim, J.; Campbell, A. S.; de Ávila, B. E.-F.; Wang, J. Wearable biosensors for healthcare monitoring. *Nat. Biotechnol.* **2019**, *37*, 389–406
- (14) Bariya, M.; Nyein, H. Y. Y.; Javey, A. Wearable sweat sensors. *Nat. Electron.* **2018**, *1*, 160–171.
- (15) Choi, J.; Ghaffari, R.; Baker, L. B.; Rogers, J. A. Skin-interfaced systems for sweat collection and analytics. *Sci. Adv.* **2018**, *4*, No. eaar3921.
- (16) Scallan, J.; Huxley, V. H.; Korthuis, R. J. Capillary Fluid Exchange: Regulation, Functions, and Pathology; Morgan & Claypool Life Sciences Publishers: San Rafael (CA), 2010.
- (17) Samant, P. P.; Prausnitz, M. R. Mechanisms of sampling interstitial fluid from skin using a microneedle patch. *Proc. Natl. Acad. Sci. U.S.A.* **2018**, *115*, 4583–4588.
- (18) Heikenfeld, J.; Jajack, A.; Feldman, B.; Granger, S. W.; Gaitonde, S.; Begtrup, G.; Katchman, B. A. Accessing analytes in biofluids for peripheral biochemical monitoring. *Nat. Biotechnol.* **2019**, 37, 407–419.
- (19) Samant, P. P.; Niedzwiecki, M. M.; Raviele, N.; Tran, V.; Mena-Lapaix, J.; Walker, D. I.; Felner, E. I.; Jones, D. P.; Miller, G. W.; Prausnitz, M. R. Sampling interstitial fluid from human skin using a microneedle patch. *Sci. Transl. Med.* **2020**, *12*, No. eaaw0285.
- (20) Miller, P. R.; Taylor, R. M.; Tran, B. Q.; Boyd, G.; Glaros, T.; Chavez, V. H.; Krishnakumar, R.; Sinha, A.; Poorey, K.; Williams, K. P.; Branda, S. S.; Baca, J. T.; Polsky, R. Extraction and biomolecular analysis of dermal interstitial fluid collected with hollow microneedles. *Commun. Biol.* 2018, 1, 173.
- (21) Kool, J.; Reubsaet, L.; Wesseldijk, F.; Maravilha, R. T.; Pinkse, M. W.; D'Santos, C. S.; van Hilten, J. J.; Zijlstra, F. J.; Heck, A. J. R. Suction blister fluid as potential body fluid for biomarker proteins. *Proteomics* **2007**, *7*, 3638–3650.
- (22) Kim, J.; Sempionatto, J. R.; Imani, S.; Hartel, M. C.; Barfidokht, A.; Tang, G.; Campbell, A. S.; Mercier, P. P.; Wang, J. Simultaneous Monitoring of Sweat and Interstitial Fluid Using a Single Wearable Biosensor Platform. *Adv. Sci.* **2018**, *5*, 1800880.
- (23) Kiistala, U. Suction Blister Device for Separation of Viable Epidermis from Dermis*. *J. Invest. Dermatol.* **1968**, *50*, 129–137.
- (24) Madden, J.; O'Mahony, C.; Thompson, M.; O'Riordan, A.; Galvin, P. Biosensing in dermal interstitial fluid using microneedle based electrochemical devices. *Sens. Biosens. Res.* **2020**, *29*, 100348.
- (25) Parrilla, M.; Cuartero, M.; Padrell Sánchez, S.; Rajabi, M.; Roxhed, N.; Niklaus, F.; Crespo, G. A. Wearable All-Solid-State Potentiometric Microneedle Patch for Intradermal Potassium Detection. *Anal. Chem.* **2019**, *91*, 1578–1586.
- (26) Ventrelli, L.; Marsilio Strambini, L.; Barillaro, G. Microneedles for Transdermal Biosensing: Current Picture and Future Direction. *Adv. Healthcare Mater.* **2015**, *4*, 2606–2640.
- (27) Wang, Z.; Luan, J.; Seth, A.; Liu, L.; You, M.; Gupta, P.; Rathi, P.; Wang, Y.; Cao, S.; Jiang, Q.; Zhang, X.; Gupta, R.; Zhou, Q.; Morrissey, J. J.; Scheller, E. L.; Rudra, J. S.; Singamaneni, S. Microneedle patch for the ultrasensitive quantification of protein biomarkers in interstitial fluid. *Nat. Biomed. Eng.* **2021**, *5*, 64–76.
- (28) Zhang, X.; Chen, G.; Bian, F.; Cai, L.; Zhao, Y. Encoded Microneedle Arrays for Detection of Skin Interstitial Fluid Biomarkers. *Adv. Mater.* **2019**, *31*, 1902825.
- (29) Miller, P. R.; Xiao, X.; Brener, I.; Burckel, D. B.; Narayan, R.; Polsky, R. Microneedle-Based Transdermal Sensor for On-Chip Potentiometric Determination of K⁺. *Adv. Healthcare Mater.* **2014**, 3, 876–881.
- (30) Whang, R.; Oei, T. O.; Aikawa, J. K.; Watanabe, A.; Vannatta, J.; Fryer, A.; Markanich, M. Predictors of Clinical Hypomagnesemia. *Arch. Intern. Med.* **1984**, 144, 1794–1796.
- (31) Weglicki, W.; Quamme, G.; Tucker, K.; Haigney, M.; Resnick, L. Potassium, magnesium, and electrolyte imbalance and complications in disease management. *Clin. Exp. Hypertens.* **2005**, *27*, 95–112.
- (32) Adlin, E. V.; Marks, A. D.; Channick, B. J. The salivary sodium/potassium ratio in hypertension: relation to race and plasma renin activity. *Clin. Exp. Hypertens., Part A* **1982**, *4*, 1869–1880.

- (33) Adlin, E. V.; Channick, B. J.; Marks, A. D. Salivary sodium-potassium ratio and plasma renin activity in hypertension. *Circulation* **1969**, 39, 685–692.
- (34) Randall, H. T. Fluid, electrolyte, and acid-base balance. Surg. Clin. North Am. 1976, 56, 1019–1058.
- (35) Bollella, P.; Sharma, S.; Cass, A. E. G.; Antiochia, R. Minimally-invasive Microneedle-based Biosensor Array for Simultaneous Lactate and Glucose Monitoring in Artificial Interstitial Fluid. *Electroanalysis* **2019**, *31*, 374–382.
- (36) Bollella, P.; Sharma, S.; Cass, A. E. G.; Antiochia, R. Microneedle-based biosensor for minimally-invasive lactate detection. *Biosens. Bioelectron.* **2019**, *123*, 152–159.
- (37) Lee, Y.; Howe, C.; Mishra, S.; Lee, D. S.; Mahmood, M.; Piper, M.; Kim, Y.; Tieu, K.; Byun, H.-S.; Coffey, J. P.; Shayan, M.; Chun, Y.; Costanzo, R. M.; Yeo, W.-H. Wireless, intraoral hybrid electronics for real-time quantification of sodium intake toward hypertension management. *Proc. Natl. Acad. Sci. U.S.A.* **2018**, *115*, 5377–5382.
- (38) Ferlauto, L.; D'Angelo, A. N.; Vagni, P.; Airaghi Leccardi, M. J. I.; Mor, F. M.; Cuttaz, E. A.; Heuschkel, M. O.; Stoppini, L.; Ghezzi, D. Development and Characterization of PEDOT:PSS/Alginate Soft Microelectrodes for Application in Neuroprosthetics. *Front. Neurosci.* 2018, 12, 648.
- (39) Emaminejad, S.; Gao, W.; Wu, E.; Davies, Z. A.; Yin Nyein, H.; Challa, S.; Ryan, S. P.; Fahad, H. M.; Chen, K.; Shahpar, Z.; Talebi, S.; Milla, C.; Javey, A.; Davis, R. W. Autonomous sweat extraction and analysis applied to cystic fibrosis and glucose monitoring using a fully integrated wearable platform. *Proc. Natl. Acad. Sci. U.S.A.* **2017**, *114*, 4625–4630.
- (40) Bandodkar, A. J.; Molinnus, D.; Mirza, O.; Guinovart, T.; Windmiller, J. R.; Valdés-Ramírez, G.; Andrade, F. J.; Schöning, M. J.; Wang, J. Epidermal tattoo potentiometric sodium sensors with wireless signal transduction for continuous non-invasive sweat monitoring. *Biosens. Bioelectron.* **2014**, *54*, 603–609.
- (41) Gao, W.; Emaminejad, S.; Nyein, H. Y. Y.; Challa, S.; Chen, K.; Peck, A.; Fahad, H. M.; Ota, H.; Shiraki, H.; Kiriya, D.; Lien, D.-H.; Brooks, G. A.; Davis, R. W.; Javey, A. Fully integrated wearable sensor arrays for multiplexed in situ perspiration analysis. *Nature* **2016**, *529*, 509–514.
- (42) Zhai, Q.; Yap, L. W.; Wang, R.; Gong, S.; Guo, Z.; Liu, Y.; Lyu, Q.; Wang, J.; Simon, G. P.; Cheng, W. Vertically Aligned Gold Nanowires as Stretchable and Wearable Epidermal Ion-Selective Electrode for Noninvasive Multiplexed Sweat Analysis. *Anal. Chem.* **2020**, *92*, 4647–4655.
- (43) Nyein, H. Y. Y.; Bariya, M.; Kivimäki, L.; Uusitalo, S.; Liaw, T. S.; Jansson, E.; Ahn, C. H.; Hangasky, J. A.; Zhao, J.; Lin, Y.; Happonen, T.; Chao, M.; Liedert, C.; Zhao, Y.; Tai, L.-C.; Hiltunen, J.; Javey, A. Regional and correlative sweat analysis using high-throughput microfluidic sensing patches toward decoding sweat. *Sci. Adv.* 2019, 5, No. eaaw9906.
- (44) Mousavi, M. P. S.; Ainla, A.; Tan, E. K. W.; Abd El-Rahman, M. K.; Yoshida, L.; Yuan, L.; Sigurslid, H. H.; Arkan, N.; Yip, M. C.; Abrahamsson, C. K.; Homer-Vanniasinkam, S.; Whitesides, G. M. Ion sensing with thread-based potentiometric electrodes. *Lab Chip* **2018**, 18, 2279–2290.
- (45) Rich, M.; Mendecki, L.; Mensah, S. T.; Blanco-Martinez, E.; Armas, S.; Calvo-Marzal, P.; Radu, A.; Chumbimuni-Torres, K. Y. Circumventing Traditional Conditioning Protocols in Polymer Membrane-Based Ion-Selective Electrodes. *Anal. Chem.* **2016**, *88*, 8404–8408.
- (46) Rose, D. P.; Ratterman, M. E.; Griffin, D. K.; Hou, L.; Kelley-Loughnane, N.; Naik, R. R.; Hagen, J. A.; Papautsky, I.; Heikenfeld, J. C. Adhesive RFID Sensor Patch for Monitoring of Sweat Electrolytes. *IEEE Trans. Biomed. Eng.* **2015**, *62*, 1457–1465.
- (47) Lim, H.-R.; Lee, Y.; Jones, K. A.; Kwon, Y.-T.; Kwon, S.; Mahmood, M.; Lee, S. M.; Yeo, W.-H. All-in-one, wireless, fully flexible sodium sensor system with integrated Au/CNT/Au nanocomposites. Sens. Actuators, B 2021, 331, 129416.
- (48) Guinovart, T.; Crespo, G. A.; Rius, F. X.; Andrade, F. J. A reference electrode based on polyvinyl butyral (PVB) polymer for

- decentralized chemical measurements. Anal. Chim. Acta 2014, 821, 72-80.
- (49) Zdrachek, E.; Bakker, E. Potentiometric sensing. *Anal. Chem.* **2020**, 93, 72–102.
- (50) Shao, Y.; Ying, Y.; Ping, J. Recent advances in solid-contact ion-selective electrodes: functional materials, transduction mechanisms, and development trends. *Chem. Soc. Rev.* **2020**, *49*, 4405–4465.
- (51) Bobacka, J.; Ivaska, A.; Lewenstam, A. Potentiometric ion sensors. *Chem. Rev.* **2008**, *108*, 329–351.
- (52) Ghosh, T.; Chung, H. J.; Rieger, J. All-Solid-State Sodium-Selective Electrode with a Solid Contact of Chitosan/Prussian Blue Nanocomposite. *Sensors* **2017**, *17*, 2536.
- (53) Ialongo, C.; Bernardini, S. Phlebotomy, a bridge between laboratory and patient. *Biochem. Med.* **2016**, *26*, 17–33.
- (54) Sensor needle gauge sizes: Dexcom 26 gauge, A. N. g., Medtronic Paradigm REAL Time Revel 23 gauge., Based on Diabetes Health 2008, 2008; Vol. 09; pp 28–29.
- (55) Cánovas, R.; Padrell Sánchez, S.; Parrilla, M.; Cuartero, M.; Crespo, G. A. Cytotoxicity Study of Ionophore-Based Membranes: Toward On-Body and in Vivo Ion Sensing. ACS Sens. 2019, 4, 2524–2535.
- (56) Dervisevic, M.; Alba, M.; Prieto-Simon, B.; Voelcker, N. H. Skin in the diagnostics game: Wearable biosensor nano- and microsystems for medical diagnostics. *Nano Today* **2020**, *30*, 100828.
- (57) Hu, J.; Stein, A.; Bühlmann, P. Rational design of all-solid-state ion-selective electrodes and reference electrodes. *TrAC, Trends Anal. Chem.* **2016**, 76, 102–114.
- (58) Bakker, E. Can calibration-free sensors be realized? ACS Sens. 2016, 1, 838–841.
- (59) Teymourian, H.; Tehrani, F.; Mahato, K.; Wang, J. Lab under the Skin: Microneedle Based Wearable Devices. *Adv. Healthcare Mater.* **2021**, No. e2002255.
- (60) García-Guzmán, J. J.; Pérez-Ràfols, C.; Cuartero, M.; Crespo, G. A. Toward In Vivo Transdermal pH Sensing with a Validated Microneedle Membrane Electrode. ACS Sens. 2021, 6, 1129–1137.
- (61) Zhao, X.; Chen, X.; Yuk, H.; Lin, S.; Liu, X.; Parada, G. Soft Materials by Design: Unconventional Polymer Networks Give Extreme Properties. *Chem. Rev.* **2021**, *121*, 4309–4372.
- (62) Pawlak, M.; Bakker, E. Chemical Modification of Polymer Ion-Selective Membrane Electrode Surfaces. *Electroanalysis* **2014**, *26*, 1121–1131.
- (63) Hernández-Neuta, I.; Neumann, F.; Brightmeyer, J.; Ba Tis, T.; Madaboosi, N.; Wei, Q.; Ozcan, A.; Nilsson, M. Smartphone-based clinical diagnostics: towards democratization of evidence-based health care. *J. Intern. Med.* **2019**, 285, 19–39.